Since January 2020 Elsevier has created a COVID-19 resource centre with free information in English and Mandarin on the novel coronavirus COVID-19. The COVID-19 resource centre is hosted on Elsevier Connect, the company's public news and information website.

Virus Research 321 (2022) 198915

Contents lists available at ScienceDirect

Virus Research

journal homepage: www.elsevier.com/locate/virusres

Identification of hACE2-interacting sites in SARS-CoV-2 spike receptor binding domain for antiviral drugs screening

Xiaopeng Hu [a,1], Jiahua Cui [b,1], Jun Chen [c,1], Shujuan Du [d], Xinyu Wang [d], Yabin Zhang [a], Jiajun Qian [b], Haifeng Chen [c], Fang Wei [e,*], Qiliang Cai [d,*], Jinping Jia [b,*], Ji Wu [a,*]

[a] Renji Hospital, Key Laboratory for the Genetics of Developmental and Neuropsychiatric Disorders, Ministry of Education, Bio-X Institutes, School of Medicine, Shanghai Jiao Tong University, Shanghai 200240, China
[b] School of Chemistry and Chemical Engineering, Shanghai Jiaotong University, China
[c] Key Laboratory of Microbial Metabolism, Department of Bioinformatics and Biostatistics, National Experimental Teaching Center for Life Sciences and Biotechnology, College of Life Sciences and Biotechnology, Shanghai Jiao Tong University, Shanghai 200240, China
[d] MOE & MOH Key Laboratory of Medical Molecular Virology, School of Basic Medicine, Shanghai Medical College, Fudan University, Shanghai 200032, China
[e] Sheng Yushou Center of Cell Biology and Immunology, Joint International Research Laboratory of Metabolic & Developmental Sciences, School of Life Sciences and Biotechnology, Shanghai Jiaotong University, Shanghai 200032, China

ARTICLE INFO

Keywords:
SARS-CoV-2
RBD
binding sites
Cephalosporin derivative
Cefixime
Ceftazidime

ABSTRACT

The key structure of the interface between the spike protein of Severe Acute Respiratory Syndrome Coronavirus 2 (SARS-CoV-2) and human angiotensin-converting enzyme 2 (hACE2) acts as an essential switch for cell entry by the virus and drugs targets. However, this is largely unknown. Here, we tested three peptides of spike receptor binding domain (RBD) and found that peptide 391–465 aa is the major hACE2-interacting sites in SARS-CoV-2 spike RBD. We then identified essential amino acid residues (403R, 449Y, 454R) of peptide 391–465 aa that were critical for the interaction between the RBD and hACE2. Additionally, a pseudotyped virus containing SARS-CoV-2 spike with individual mutation (R454G, Y449F, R403G, N439I, or N440I) was determined to have very low infectivity compared with the pseudotyped virus containing the wildtype (WT) spike from reference strain Wuhan 1, respectively. Furthermore, we showed the key amino acids had the potential to drug screening. For example, molecular docking (Docking) and infection assay showed that Cephalosporin derivatives can bind with the key amino acids to efficiently block infection of the pseudoviruses with wild type spike or new variants. Moreover, Cefixime inhibited live SARS-CoV-2 infection. These results also provide a novel model for drug screening and support further clinical evaluation and development of Cephalosporin derivatives as novel, safe, and cost-effective drugs for prevention/treatment of SARS-CoV-2.

1. Introduction

Coronavirus 2019 (COVID-19) is caused by a new SARS-like coronavirus (SARS-CoV-2) that is highly transmissible from person-to-person (Li et al., 2020; Huang et al., 2020). COVID-19 can cause severe aspiration syndrome, multiple organ damage, and death in humans (Huang et al., 2020; Chan et al., 2020; Sohrabi et al., 2020; Lv et al., 2020; Yang et al., 2020). According to publicly available datasets on various online platforms, more than 480 million people have been diagnosed, and nearly 6.2 million have died between late December 2019 and Mar 2022. As SARS-CoV-2 continues to mutate and escape the immune system, people infected with SARS-CoV-2 are also infected with the variants, and the vaccine cannot fully block the infection of the virus, Therefore, additional methods for the prevention and control of COVID-19 epidemic are urgently needed.

For developing such tools, it is critical to understand the SARS-CoV-2 receptor-recognition mechanism, which regulates the infectivity, pathogenic mechanism, and host range of the virus (Perlman and Netland, 2009; Li, 2016). Spike glycoprotein on the surface of SARS-CoV-2 mediates receptor recognition and membrane fusion (Li, 2016; Bosch et al., 2003). This glycoprotein is 1273 amino acids long and comprises a distinct N-terminal domain, receptor-binding domain (RBD), subdomains 1 and 2, transmembrane domain, C-terminal domain with heptad repeats 1 and 2, and a cytoplasmic tail (Wrapp et al., 2020).

* Corresponding authors.
E-mail addresses: fangwei@sjtu.edu.cn (F. Wei), qiliang@fudan.edu.cn (Q. Cai), jpjia@sjtu.edu.cn (J. Jia), jiwu@sjtu.edu.cn (J. Wu).
[1] These authors have contributed equally to this work.

https://doi.org/10.1016/j.virusres.2022.198915
Received 25 May 2022; Received in revised form 1 September 2022; Accepted 5 September 2022
Available online 6 September 2022

SARS-CoV-2 spike glycoprotein attaches to human angiotensin-converting enzyme 2 (hACE2) to infect host cells (Wang et al., 2020; Letko et al., 2020). The spike S1 subunit contains a RBD, which directly binds to the peptidase domain of hACE2 (hACE2-PD), while the spike S2 subunit is responsible for membrane fusion (Hoffmann et al., 2020; Walls et al., 2020). When the spike S1 subunit binds to the host receptor, the restriction site on the spike S2 subunit is exposed and cleaved by the host protease: Recombinant Transmembrane Protease, Serine 2 (TMPRSS2), a process that is critical for viral infection (Hoffmann et al., 2020; Walls et al., 2020). Additionally, during viral infection, the host protease cleaves the spike protein trimers into subunits S1 and S2 (Hoffmann et al., 2020; Walls et al., 2020).

The recently published crystal structure of the SARS-CoV-2 spike RBD complexed with hACE2 revealed some apparent binding sites between the spike RBD and hACE2-PD (Wrapp et al., 2020; Shang et al., 2020; Yan et al., 2020). Additionally, some hydrogen bonds between spike RBD and hACE2-PD were predicted by bioinformatics, and polar interactions between spike RBD and hACE2 are thought to contribute heavily to viral infectivity (Wang et al., 2020; Yan et al., 2020; Chowdhury et al., 2020) . N-glycosylation at specific sites of SARS-CoV-2 spike glycoprotein was also believed to affect viral infectivity and antibody-mediated neutralization (Li et al., 2020). Although a few studies revealed some key amino acids in the binding sites between SARS-CoV-2 spike RBD and hACE2-PD (Yi et al., 2020), these binding sites have not been fully elucidated.

SARS-CoV-2 is a positive-stranded RNA virus. Its genome is approximately 80% homologous with the SARS-CoV-1 genome and approximately 96% homologous with the genome of the bat coronavirus RaTG13, which appears to be the closest relative of SARS-CoV-2 (Zhou et al., 2020). The genome differences between RaTG13 and SARS-CoV-2 may have played a critical role in the binding sites (between SARS-CoV-2 spike RBD and hACE2-PD) and infectivity of SARS-CoV-2. However, this is also largely unknown.

The key amino acid sites of SARS-CoV-2 spike (binding sites to hACE2) may be potential targets for neutralizing antibodies and small molecule drugs, and should be identified. Although potent neutralizing antibodies, inhibitors, as well as soluble ACE2 blocking SARS-CoV-2 entry into cells were reported (Baum et al., 2020; Ju et al., 2020; Pinto et al., 2020; Chan et al., 2020; Pan et al., 2021; Liu et al., 2021), there is still a need for non-toxic, good drug properties of small molecular compounds as another effective way to prevent and intervene SARS-CoV-2 infection.

7-Amino cephalosporanic acid is the core structure scaffold for the preparation of cephalosporin antibiotics and related intermediates. Due to the poor antibiotic activity, it has not been used for the treatment of infectious diseases in clinics. Cefprozil as the orally active second-generation cephalosporins could be used to treat of upper respiratory tract infection and bronchitis. Ceftazidime and Cefixime were the third generation cephalosporin antibiotics, which were generally prescribed to treat several bacterial infections. Ceftazidime is used to treat infections of lower respiratory tract, skin, urinary tract, blood-stream, joint, and abdominal (Shirley, 2018). Cefixime is prescribed for bacterial infections of the chest, ears, urinary tract, and throat (tonsilitis and pharyngitis), uncomplicated gonorrhea, upper and lower respiratory tract infections, acute otitis media, and gonococcal urethritis (Quintiliani, 1996; Bluestone, 1993; Arthur et al., 1996). Ceftazidime has been identified as an inhibitor towards the wild type SARS-CoV-2 S proein-ACE2 interactions in recent studies (Lin et al., 2021). However, its action towards specific variants has not been tested. Cefixime was tested by the computational studies to be used as potent inhibitors of COVID-19 (Rashid et al., 2022). However, these in silico docking results had not been confirmed by *in vitro* and *in vivo* cell-infection studies.

Here, we identified which part of the SARS-CoV-2 spike RBD is the major hACE2-interacting sites in SARS-CoV-2 spike RBD and further investigated which essential amino acid residues of this part are critical for the binding of SARS-CoV-2 spike to hACE2, which determined to the infectivity of SARS-CoV-2. Furthermore, we investigated whether Cephalosporin derivatives can inhibit SARS-CoV-2 spike (WT and variants)-mediated infection by binding with the key amino acids for interaction between Spike RBD and hACE2.

2. Materials and methods

2.1. Compounds

All tested compounds were purchased from National Institutes for Food and Drug Control in China (> 98% pure by HPLC analysis).

2.2. Cell line

The 293T-hACE2 cell line was generated by infecting 293T cells (*Homo sapiens*, embryonic kidney) (Thermo scientific) with a lentivirus containing hACE2- and TMPRSS2-expressing plasmids. These cells stably expressed TMPRSS2 and 3 × Flag-hACE2.

2.3. Site-directed mutagenesis

The plasmid containing the gene for SARS-CoV-2 spike protein containing mutations (GenBank: MN_908947) were generated by using pHCMV-2019-nCov-S (OBiO Technology Corp., Ltd.) as the template. Briefly, the mutant SARS-CoV-2 spike sequences were obtained by applying site-directed mutant PCR and overlap PCR. The sequences containing the spike mutation were then cloned into the pHCMV plasmid. The remnant strain was used to directly transform *Escherichia coli* DH5α competent cells; single clones were selected, and then Sanger sequenced.

The mutant SARS-CoV-2 spike RBD sequences were obtained by applying site-directed mutant PCR and overlap PCR. The sequences containing the spike RBD or mutations were then cloned into the plasmid pGEX-4T-1 or PCDNA3.1. The resulting recombinant donor plasmids were used to transform *E. coli* BL21 or DH5α competent cells; single clones for each mutation were selected, and then Sanger sequenced. Primer information is listed in Table S1.

2.4. Plasmid transfection and protein purification

The 293T cell or 293T-hACE2 cell line was transfected with PCDNA3.1 containing spike RBD individual mutation or pHCMV-2019-nCov-S containing SARS-CoV-2 spike protein individual mutation by using lipo8000 (Beyotime) for 24 h, according to the manufacturer's instruction. At 72 h after transfection, the cells were screened with Puromycin.

The 293T-hACE2 cell line or 293T cell transfected with PCDNA3.1 containing 3x FLAG-spike RBD (individual mutation or WT) were lysed by Radio-Immunoprecipitation Assay (RIPA) Buffer and the total protein were centrifugally collected. The hACE2 and Spike RBD (individual mutation or WT) were then purified by Anti-Flag Affinity gel, according to the manufacturer's instruction.

2.5. GST pull-down assays

The GST pull-down assays were performed as described previously (Bain et al., 2017). Briefly, the expression of GST-fusion proteins was induced in *E. coli* BL21 transformed with the recombinant plasmid pGEX-4T-1 by shaking with 0.1 mM Isopropyl β-D-Thiogalactoside (IPTG) (Sangon) at 16 °C overnight. The bacteria were then collected *via* centrifugation (10,000 × *g* RCF) for 15 min at 4 °C. The resulting bacterial pellets were thoroughly resuspended in PBST (sterile PBS containing 10% Triton X-100 and 1 mM PMSF) and transferred into 30 ml tubes. The cells were then sonicated with a Branson sonifier on ice until the resulting lysates were clear. The lysates were centrifuged at 20,000 × *g* for 20 min at 4 °C, after which the resulting supernatants were

transferred to fresh tubes along with prewashed Glutathione-Sepharose beads (Thermo scientific). The tubes were then rotated for 4 h at 4 °C. After magnetic shelves were used to collect beads, the beads were washed three times with PBST. The washed beads were then mixed with lysates of 293T cells that stably expressed 3 × Flag-hACE2 and were lysed with RIPA buffer (Beyotime). The tubes were then rotated overnight at 4 °C. Magnetic shelves were used to collect beads, after which the beads were again washed three times with PBST. RIPA buffer containing 5 × loading buffer (Beyotime; 40 μl) was added to the beads, and they were boiled for 10 min. Magnetic shelves were used to remove the beads and collect the supernatants.

2.6. SDS-PAGE and western blot

The pull-down samples and 1% of the input or cell lysis were loaded on a 10% sodium dodecyl sulfate polyacrylamide gel electrophoresis (SDS-PAGE) gel (Bain et al., 2017). After the contents of the SDS-PAGE gels were transferred polyvinylidene fluoride (PVDF) membranes using standard procedures, the membranes were blocked in TBST (Tris-Buffered Saline and Tween 20) containing 5% non-fat milk powder for 1 h at room temperature. The membranes were then incubated with anti-GST (Santa Cruz), anti-His(Cell Signal Technology) or anti-Flag (Sigma) antibody overnight at 4 °C and washed three times with TBST. The membranes were subsequently incubated with horseradish peroxidase (HRP)-conjugated secondary antibody (Proteintech) for 1 h at room temperature, and bands were detected with enhanced chemiluminescence (ECL; Yeasen). The resulting images were screened by using a chemiluminescence imaging system (ProteinSimple).

2.7. Immunofluorescence assay

For immunofluorescence, cells were fixed with 4% paraformaldehyde (PFA) in PBS (pH 7.4) for 30 min, washed three times with PBS, followed by incubation with 0.5% Triton X-100 in PBS for 10 min. Then cells were blocked with 5% goat serum in PBS for 30 min at room temperature, and then incubated with primary antibodies diluted in PBS at 4 °C overnight. Primary antibodies were diluted with PBS as below: Flag (1:50), His (1:50) and after incubation finish, the cells were washed with PBS and then incubated with goat anti-mouse IgG-FITC and goat anti-rabbit IgG-TRITC secondary antibodies (1:200; Invitrogen) at room temperature, followed by washes and staining with 4′, 6-diamidino-2-phenlindole dihydrochloride (DAPI).

2.8. Surface plasmon resonance analysis

SPR-based measurements were performed by Biacore (8 K). Briefly, WT RBD, R454G RBD, Y449F RBD or R403G RBD were immobilized to a CM5 sensorchip (Cytiva) to a level of around 200 response units (RUs) using Biacore (8 K). For affinity analysis, hACE2 was dissolved in HBS-ET running buffer at concentrations of 0.78, 1.56, 3.125, 6.25, 12.5, 25 μg/m (Cefixime was dissolved in PBS supplement with 0.05% Tween-20 and 5% DMSO at concentrations of 15.6, 31.25, 62.5, 125 μM) and were run across the chip. Each sample that was bound to the antigen surface was dissociated by HBS-ET buffer (or PBS supplement with 0.05% Tween-20 and 5% DMSO) for 120 s at a flow rate of 30 μl/min. Regeneration of sensor chips was performed for 30 s using regeneration buffer (glycine pH 2.0). The dissociation constant (KD) was determined and recorded by Biacore (Cytiva).

2.9. Molecular docking

Cephalosporin derivatives (7-Amino cephalosporanic acid, Cefprozil, Cefixime or Ceftazidime) as potential inhibitors of SARS-CoV-2 S protein-ACE2 interaction were docked into the receptor-binding domain of SARS-CoV-2 spike protein (PDB ID 6M0J) using the docking program in MOE 2008 (Cui et al., 2015; Vilar et al., 2008). Qligosaccharides and water molecules in the crystal structure were removed before the experiment. Hydrogens and partial charges were added with the protonate 3D application of MOE 2008. Site finder of MOE was employed to recognize potential binding sites on spike RBD, which were near to the receptor binding ridge on ACE2. The initial 3D conformation of Ceftazidime (1) and Cefixime (2) was optimized in ChemBio3D Ultra using MM2 energy minimization method (Sharma et al., 2009; Dong et al., 2021). For docking, we employed the default values of parameters, except for the first scoring function, where the ASE Scoring was used instead of the defaulting London dG. The best pose was characterized by the scoring results. We employed the verified molecular docking algorithm, which had been well established in the published research works that concentrated on the in silico screening of inhibitors against spike proteins using MOE software (Khelfaoui et al., 2021).

2.10. MTT assay

The cytotoxicity effect of the compounds on HEK-293T cells were measured by the standard Methyl Thiazolyl Tetrazolium (MTT) assay. Briefly, monolayers cells in 96-well plates were rinsed by PBS and incubated with indicated compounds for 48 h subsequently. Then, cells were treated with 0.5 mg/mL MTT for 4 h at 37 °C and formazan crystals in viable cells were dissolved in 150 μL DMSO. The absorbance of solubilized formazan was measured by the Synergy multimode reader (BioTek, American) at the wavelength of 490 nm.

2.11. Production of pseudotyped viruses

Pseudotyped viruses that incorporated the wildtype or point mutant spike protein from SARS-CoV-2 (GenBank: MN_908947) were constructed using a previously described procedure (Li et al., 2020; Nie et al., 2020). Briefly, when the 293T cells reached approximately 70%–80% confluence after overnight incubation, they were transfected with pHCMV-2019-nCov-S (OBiO Technology Corp., Ltd.) or a plasmid containing the sequence of the Y449F mutant spike by using Lipo8000 (Beyotime) in accordance with the manufacturer's instructions. These 293T cells were subsequently infected with G*ΔG-VSV (VSV G pseudotyped virus). After incubation at 37 °C in 5% CO_2 for 6–8 h, the cells were rinsed gently with PBS + 1% FBS, and then the cell supernatant was discarded, and then the 293T cells were cultured in fresh DMEM for 24 h. The SARS-CoV-2 pseudotyped viruses contained in the culture supernatants were then harvested, filtered (0.45 μm pore size, Millipore), and stored at −80 °C until use.

2.12. Quantification of pseudotyped virus particles

Total RNA was extracted from purified pseudotyped virus particles by using Trizol reagent (Qiagen), and then cDNA was synthesized from 1 μg of the total RNA with hiScript reverse transcriptase (Vazyme). Based on the quantification of WPRE mRNA, the pseudotyped virus particles were quantified by performing quantitative RT-PCR using FastStart Universal SYBR Green Master (Rox) and following the manufacturer's instructions.

2.13. Infection assay

Using quantitative RT-PCR, we normalized the wildtype and mutant SARS-CoV-2 spike protein pseudotyped virus particles to the same amount. The same approximate number of 293T-hACE2 cells were seeded in each well of a 96-well cell culture plate, and after overnight incubation, the cells reached 70%–80% confluence. The 293T-hACE2 cells in each well were then infected with the same amount of pseudotyped virus particles (100 μl) for 24 h. At 72 h after infection, cells were digested by trypsin. The number of EGFP-positive cells was counted by flow cytometry, and the results were used to calculate the infection ability of the pseudotyped viruses.

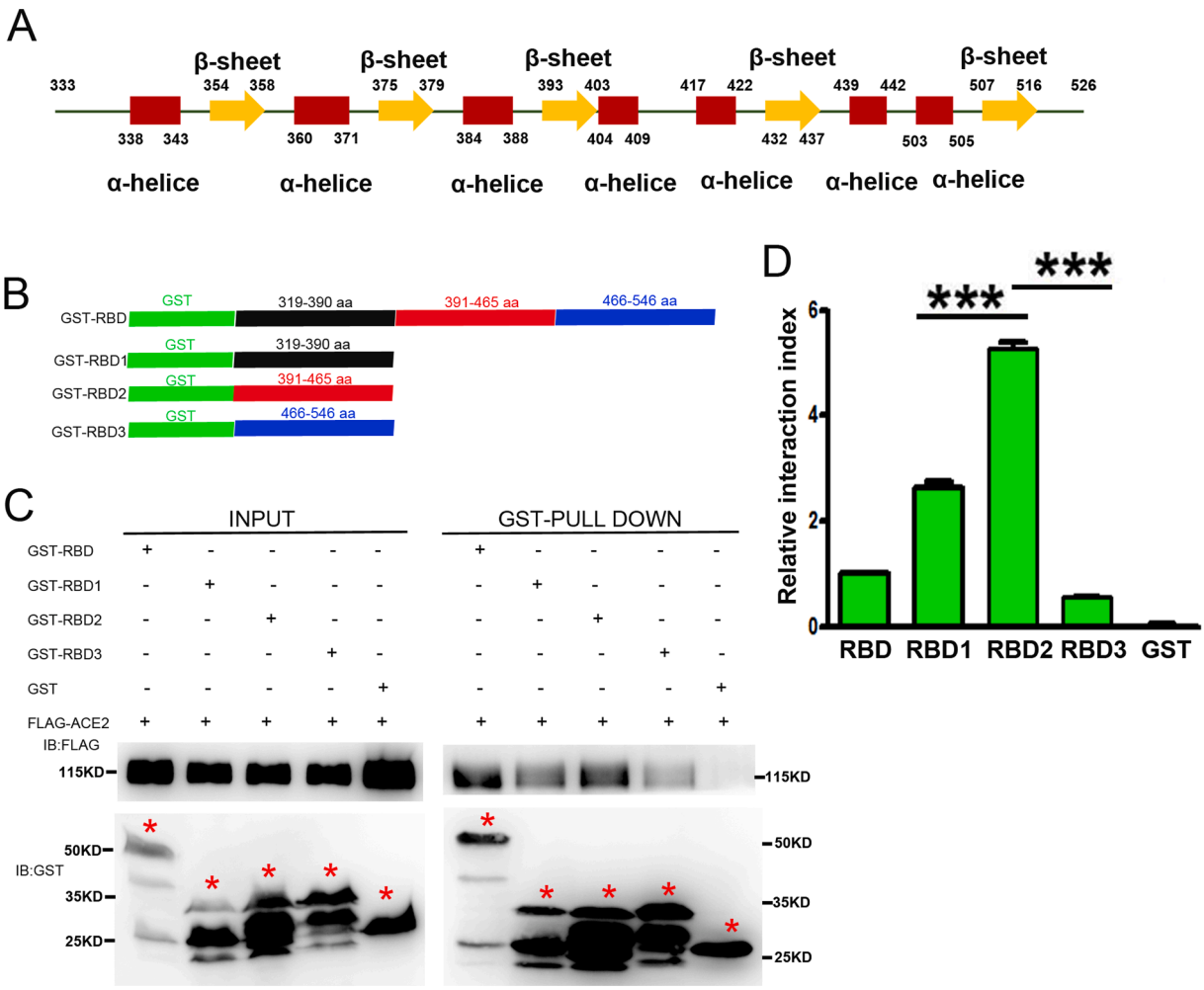

Fig. 1. *Identification of interaction between three fragments of SARS-CoV-2 spike RBD and hACE2.* (A) The Secondary structure of RBD. Arrows and rectangles indicate β sheets and α helices, respectively. (B) Three fragment plasmids of SARS-CoV-2 spike RBD were designated as GST-RBD1, GST-RBD2, and GST-RBD3. (C) The results of a GST pull-down assay assessing the interaction between GST-RBD1, GST-RBD2, or GST-RBD3 and hACE2. The asterisks represent positive bands. (D) Quantification of the relative Flag protein levels normalized to GST expression described in the GST pull-down group of (D) using image J software. ***$P < 0.001$. Bars indicate means ± s.e.m. from three independent experiments.

293T-hACE2 cells were co-incubated with or without the indicated doses of Ceftazidime (or Cefixime) and the pseudovirus bearing SARS-CoV-2 spike (WT or variants) overnight at 37 °C 5% CO_2. Then the cell supernatant was discarded, and then the 293T-hACE2 cells were cultured with or without the indicated doses of Ceftazidime (or Cefixime) for 24 h. At 72 h after infection, cells were digested by trypsin. The number of EGFP-positive cells was counted by flow cytometry, and the results were used to calculate the infection ability of the pseudotyped viruses.

To confrm the anti-SARS-CoV-2 effect of Cefixime, the Vero-E6 cells (Monkey kidney cell line) were pre-treated with Cefixime (400 μM) for 1 h, washed by PBS and then incubated with live SARS-CoV-2 and Cefixime (400 μM) in DMEM containing 2% FBS for 2 h. The cells were then washed by PBS to remove the free viruses and cultured in fresh DMEM containing 2% FBS and Cefixime (400 μM). Supernatant from live SARS-CoV-2-infected Vero-E6 cells was collected at 48 h post-infection for RNA extraction. SARS-CoV-2 copies were measured by the qRT-PCR for the viral N gene expression. Immunofluorescence assay was used to detect the expression of N protein and the result was annalysised by high content screening.

2.14. Molecular dynamics (MD) simulation

The simulations were conducted using the AMBER18 (Case et al., 2018) package with ff14SB force field (Maier et al., 2015). The initial structure of the SARS-CoV-2 spike RBD bound with hACE2 was taken from Protein Data Bank (PDB) entry 6M0J (Lan et al., 2020). Mutants in the simulations were obtained by mutating specific amino acids in the wildtype spike protein using PyMOL 2.4 software (Nag et al., 2021). Each system was set in a truncated octahedron box of a TIP3P water model with a buffer of 15 Å, and then the counter ions were added to neutralize the system. A cutoff of 8 Å was set for the van der Waals and short-range electrostatic interactions. The Partial Mesh Ewald (PME) method (Darden et al., 1993) was applied to calculate the long-range electrostatic interactions. The lengths of bonds with hydrogen atoms were constrained with the SHAKE algorithm (Ryckaert et al., 1977). All systems were minimized with 3000 steps of the steepest descent method and 3000 steps of the conjugate gradient algorithm, then heated to a temperature of 298.15 K in an NVT ensemble for 150 ps. After a 100 ps equilibration, the MD simulations were conducted in the NPT ensemble at 298.15 K for 150 ns.

For molecular dynamics simulation settings, the amber ff14SB force field is a classical force field in molecular dynamics simulations and has been validated in multiple works (Maier et al., 2015; Teixeira et al.,

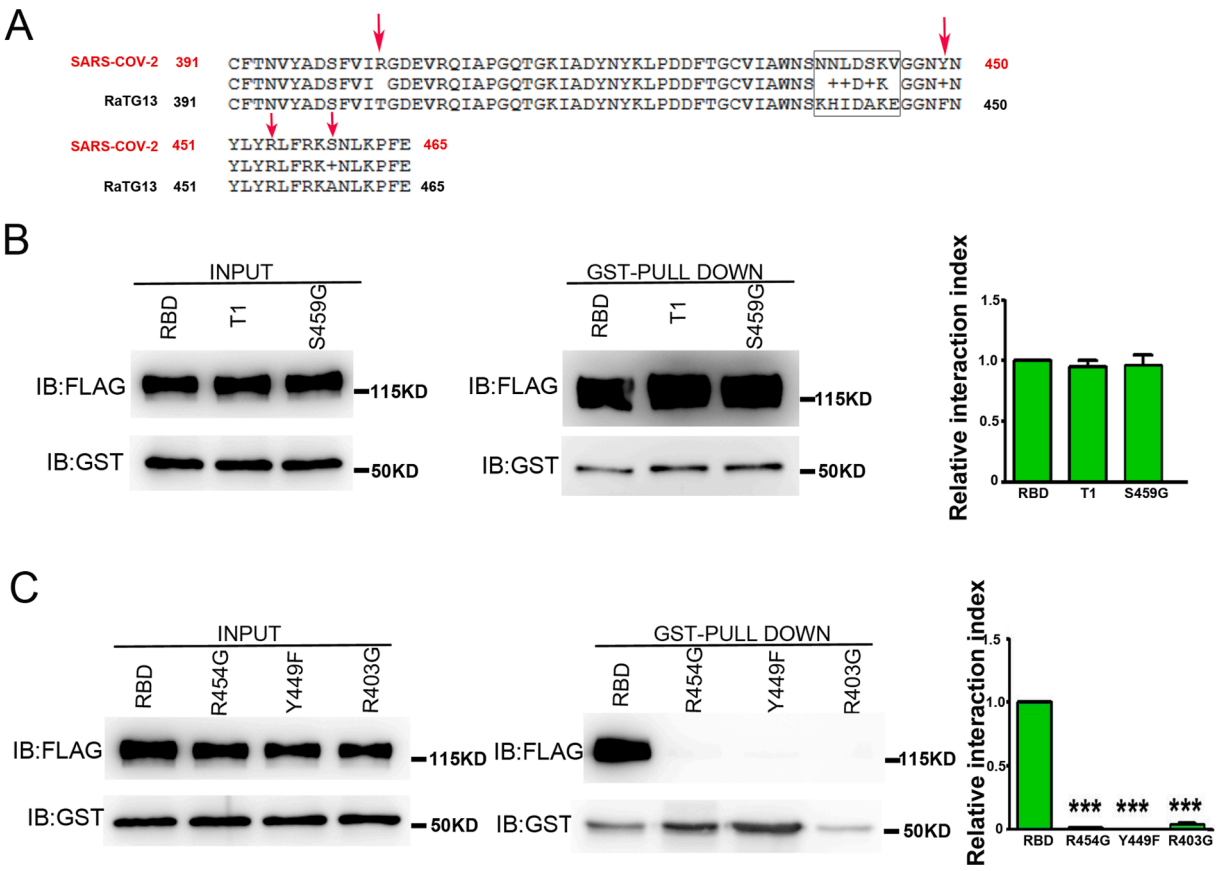

Fig. 2. Identification of the key SARS-CoV-2 spike RBD amino acid residues needed for hACE2 binding. (A) Using protein–protein BLAST, the amino acid residue differences between RBD2 and the RaTG13 spike protein sequence were detected. Arrows and the square box highlight the detected amino acid residue differences. (B) The results of a GST pull-down assay assessing the interaction between the mutant RBD GST-T1 (which contains the point mutations N439I, N440I, D442V, and K444M) or an RBD mutant domain containing the point mutation S459G and hACE2 (far left and middle panel). Quantification of the relative Flag protein levels normalized to GST expression described in the GST pull-down group of (B) using image J software (far right panel). (C) The results of a GST pull-down assay assessing the interaction between mutant RBD containing one of three individual amino acid point mutations (R454G, Y449F, or R403G) and hACE2 (far left and middle panel). Quantification of the relative Flag protein levels normalized to GST expression described in the GST pull-down group of (C) using image J software (far right panel). Bars indicate means ± s.e.m. from three independent experiments. $^{***}P < 0.001$.

2022) . Some other algorithms used by us are also recommended in the AMBER manual, such as Partial Mesh Ewald (PME) method and SHAKE algorithm (Case et al., 2018).

2.15. MD simulation data analysis

RMSDs and root mean square fluctuations (RMSFs) of Cα were analyzed with the CPPTRAJ program in AmberTools18 (Case et al., 2018; Song et al., 2017). The MMPBSA in AmberTools18 (Case et al., 2018) was used to create a compatible complex, to generate SARS-CoV-2 spike RBD and hACE2 topology files from a solvated topology file, and to calculate the total binding free energy of SARS-CoV-2 spike RBD and hACE2 (Liu et al., 2017). The calculation was based on the simulation from 50 ns to 150 ns.

2.16. Statistical analysis

To compare the differences between groups, the results were analyzed using t-tests, and values of $P < 0.05$ were considered to indicate statistical significance.

3. Results

3.1. Identifying the major hACE2-interacting sites in SARS-CoV-2 spike RBD

To identify the major hACE2-interacting sites in SARS-CoV-2 spike RBD, we first constructed three plasmids containing spike RBD fragments (GST-RBD1, GST-RBD2, and GST-RBD3) that, respectively, contain 319–390 aa, 391–465 aa, and 466–546 aa from the protein sequence of SARS-CoV-2 strain Wuhan 1 (GenBank: MN_908947) based on the secondary structure (Fig. 1A and B). The results of a GST pull-down assay show that peptide 391–465 aa are required for RBD binding (Fig. 1C and D, compare lane 3 with lanes 2 and 4). These results indicate that peptide 391–465 aa is the major hACE2-interacting sites in SARS-CoV-2 spike RBD.

3.2. Identifying the key SARS-CoV-2 spike RBD amino acid residues for hACE2 binding

Using protein–protein BLAST, we identified the following RBD2 (391–465 aa) sites that differ from the corresponding sequence in RaTG13: 403R, 439N, 440N, 449Y, and 459S (Fig. 2A). Additionally, a recent study showed N glycosylation sites, and polar amino acids may play roles in the SARS-CoV-2 spike–hACE2 interaction. Therefore, to uncover whether the identified sites and/or some polar amino acids

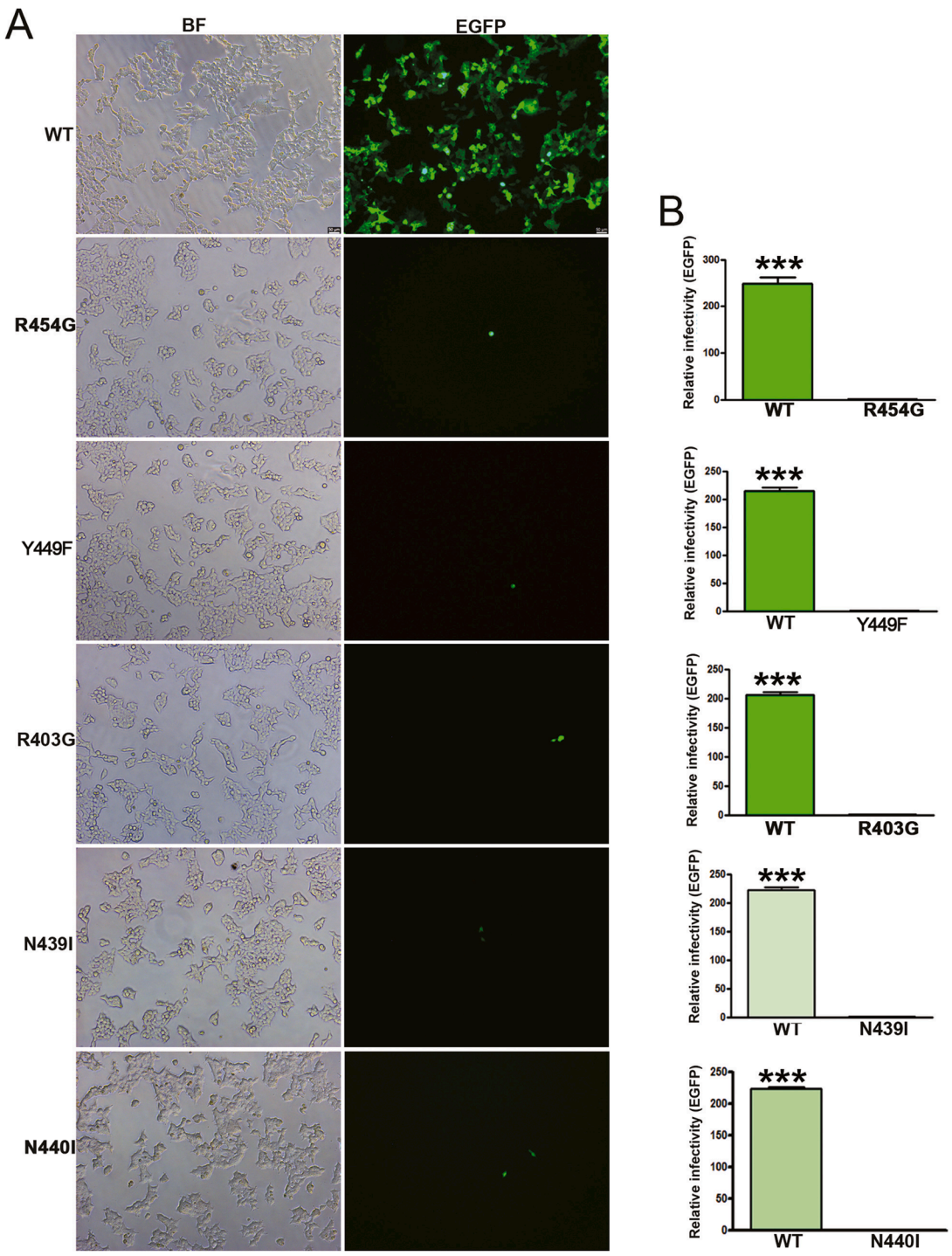

Fig. 3. Effect of SARS-CoV-2 spike RBD individual mutation on infectivity as assessed by using pseudotyped viruses. After infection with pseudotyped virus containing either wildtype SARS-CoV-2 spike RBD or the individual mutant SARS-CoV-2 spike RBD (R454G, Y449F, R403G, N439I, or N440I), EGFP-positive cells of were detected under a fluorescence microscope. (A) Representative images (Bar = 50 μm) and the number (B) of EGFP-positive cells. The relative infectivity of these pseudotyped viruses was determined based on the percentage of EGFP positivity as detected by flow cytometry, with the value for the pseudotyped virus containing the individual mutant SARS-CoV-2 spike RBD (R454G, Y449F, R403G, N439I, or N440I) set at one, respectively. *** $P < 0.001$. Bars indicate means ± s.e.m. from three independent experiments.

were essential for this interaction, we first constructed GST-T1, which contains the point mutations N439I, N440I, D442V and K444M. The results of a GST pull-down assay show that the hACE2 interaction with GST-T1 was not different from its interaction with the wildtype sequence (Fig. 2B). Moreover, we constructed GST-tagged versions of mutant spike RBD sequences carrying individual point mutations. We performed additional GST pull-down assays and found that three individual amino acid mutations (R454G, Y449F, and R403G) significantly interrupted the spike RBD–hACE2 interaction, but the individual S459G mutation did not (Fig. 2B and C). The effects of interrupting spike RBD–hACE2 interaction by three individual amino acid mutations (R454G, Y449F, and R403G) in RBD were confirmed using Surface plasmon resonance (Fig. S1). In summary, we identified three essential amino acid residues (454R, 449Y, 403R) that are critical for binding SARS-CoV-2 spike to

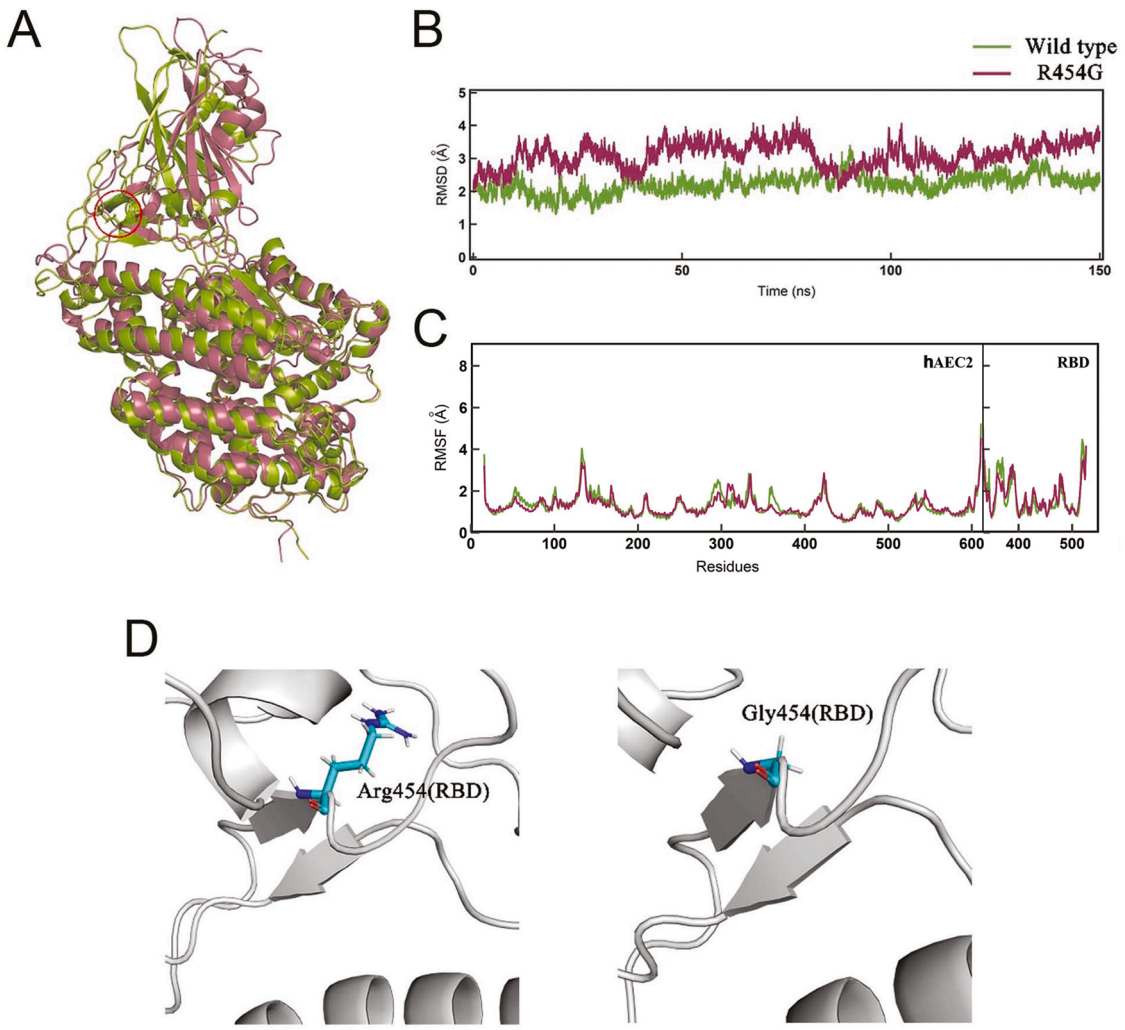

Fig. 4. *MD simulation study of affinity between SARS-CoV-2 spike RBD carrying individual mutation R454G and hACE2.* (A) Average structures in the MD simulation (150 ns). The wildtype SARS-CoV-2 spike RBD is shown in green, and the SARS-CoV-2 spike RBD R454G mutant is shown in raspberry. The RMSD between the two complexes is 2.781 Å. The mutant residues are marked with a red circle. (B, C) The RMSD (B) or RMSF (C) of Cα in the MD simulation. (D) The hydrogen bond-based interaction between SARS-CoV-2 spike R454G mutant amino acids and hACE2. In the SARS-CoV-2 spike RBD R454G mutant, no hydrogen bonds are formed with hACE2, and the total binding energy of hACE2 and RBD is −24.29 ± 0.19 kcal/mol.

hACE2.

3.3. Identification of a set of key amino acids in spike protein RBD responsible for the high infectivity of SARS-CoV-2

It is currently unknown whether the identified sites were essential for the high infectivity of SARS-CoV-2/or whether it may have increased COVID-19 transmissibility among humans. To uncover the identified sites on viral infectivity, we infected the 293T-hACE2 cell line with pseudotyped viruses containing the wildtype spike protein of SARS-CoV-2, which was derived from the spike protein sequence of SARS-CoV-2 strain Wuhan 1 (GenBank: MN_908947), or the individual mutant spike protein of SARS-CoV-2. As shown in Fig. 3, the pseudotyped virus containing spike protein with R454G, Y449F, R403G, N439I or N440I was determined to have very low infectivity, and very few cells were infected by this virus compared with virus containing wildtype spike from the reference strain Wuhan 1; the number of enhanced green fluorescent protein (EGFP)-positive cells following infection with the pseudotyped virus containing spike protein with R454G, Y449F, R403G, N439I or N440I was more than 200-fold lower than that following infection with the pseudotyped virus containing wildtype spike protein. These results suggest that spike protein 454R, 449Y, 403R, 439N and 440N were essential to the infectivity of SARS-CoV-2. The mutant Y449F spike protein has one less hydroxyl group in its structure compared with the wildtype spike protein. The above result indicates that the high infectivity of SARS-CoV-2 requires the hydrogen bond between spike 449Y and hACE2.

3.4. MD simulation study of affinity between SARS-CoV-2 spike RBD carrying individual point mutations and hACE2

We next performed a molecular dynamics (MD) simulation study of interactions between various mutant SARS-CoV-2 spike RBD carrying individual point mutations (R454G, Y449F, R403G, N439I, N440I) and hACE2, based on the published crystal structure of SARS-CoV-2 spike RBD and hACE2. For the individual point mutations, the root mean square deviation (RMSD) between R454G and wildtype was 2.781 Å (Fig. 4); the RMSD between Y449F and wildtype was 2.624 Å (Fig. 5); the RMSD between R403G and wildtype was 2.435 Å (Fig. 6); the RMSD between N439I and wildtype was 2.944 Å (Fig. S2); and the RMSD between N440I and wildtype was 2.198 Å (Fig. S3). There was a hydrogen bond between hACE2 20D and spike RBD 449Y in the wildtype, but no hydrogen bond interactions with hACE2 formed at this site for SARS-CoV-2 spike RBD point mutant Y449F (Fig. 5), which is because

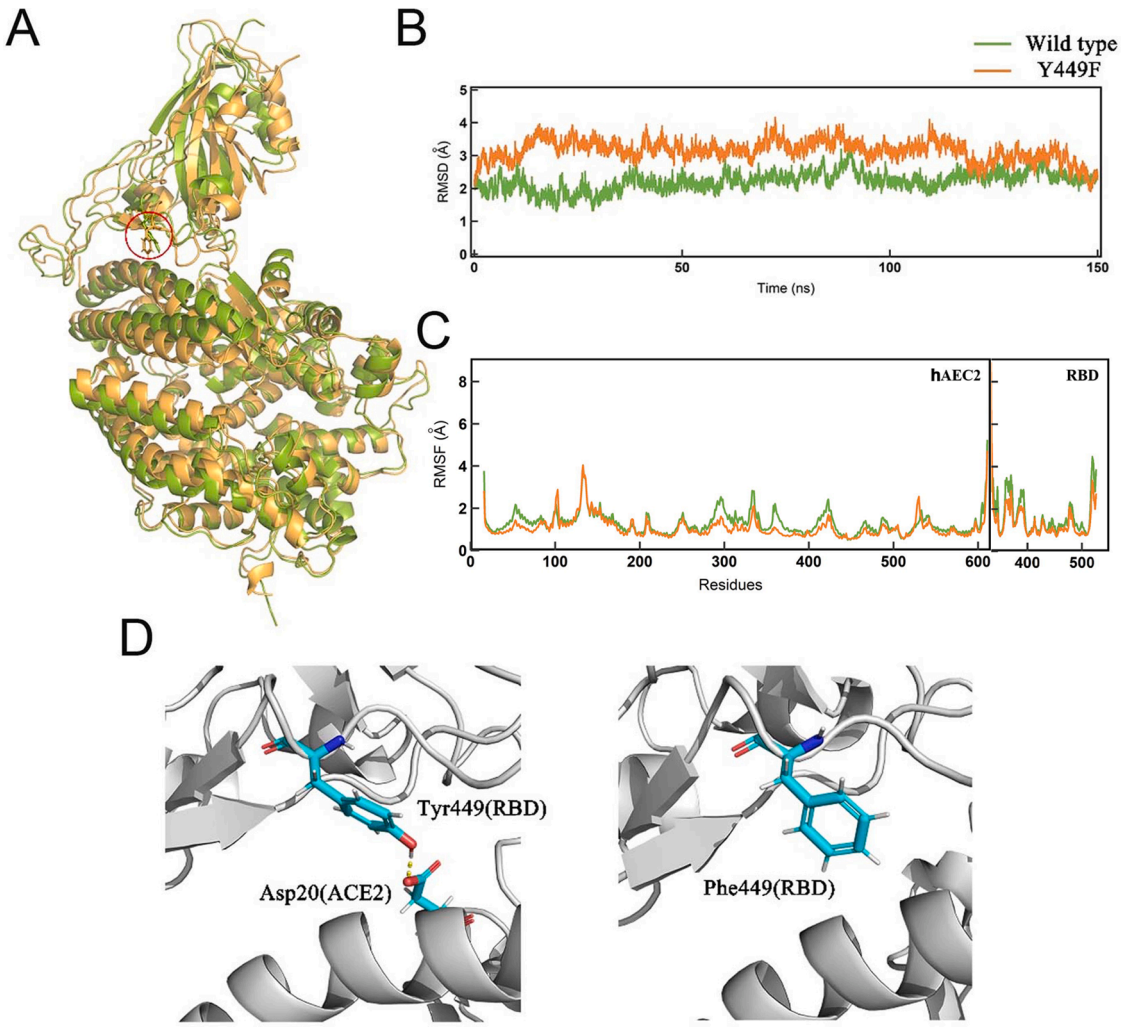

Fig. 5. *MD simulation study of affinity between SARS-CoV-2 spike RBD carrying individual mutation Y449F and hACE2.* (A) Average structures in the MD simulation (150 ns). The wildtype SARS-CoV-2 spike RBD is shown in green, and the SARS-CoV-2 spike RBD Y449F mutant is shown in orange. The RMSD between the two complexes is 2.624 Å. The mutant residues are marked with a red circle. (B, C) The RMSD (B) or RMSF (C) of Cα in the MD simulation. (D) The hydrogen bond-based interaction between SARS-CoV-2 spike RBD mutant amino acids and hACE2. In the wildtype SARS-CoV-2 spike RBD, a hydrogen bond is formed between 20D on hACE2 and 449Y on the SARS-CoV-2 spike RBD, and the total binding energy of hACE2 and wildtype SARS-CoV-2 spike RBD is −37.59 ± 0.14 kcal/mol. In the SARS-CoV-2 spike RBD Y449F mutant, no hydrogen bonds are formed with hACE2, and the total binding energy of hACE2 and the SARS-CoV-2 spike RBD Y449F mutant is −33.42 ± 0.15 kcal/mol.

phenylalanine has one less hydroxyl group on the benzene ring compared with tyrosine. In wild type, hydrogen bonds were formed between 439N and 437N, 499P, 443S, respectively (Fig. S2). The hydrogen bond with 499P disappeared in N439I mutation, and the alpha helix at the mutation site was disrupted (Fig. S2). Additionally, no hydrogen bond interactions with hACE2 were found for spike RBD 454R, 403R or 440N (Figs. 4, 6, S3), but the alpha helix at the mutation N440I site was disrupted (Fig. S3). After the individual mutations R454G, Y449F, R403G, N439I and N440I, the total binding energy of hACE2 and SARS-CoV-2 spike RBD was changed from −37.59 ± 0.14 kcal/mol to −24.29 ± 0.19 kcal/mol, from −37.59 ± 0.14 kcal/mol to −33.42 ± 0.15 kcal/mol, from −37.59 ± 0.14 kcal/mol to −33.41 ± 0.24 kcal/mol, from −37.59 ± 0.14 kcal/mol to -24.99 ± 0.51 kcal/mol and from −37.59 ± 0.14 kcal/mol to -40.51 ± 0.54 kcal/mol, respectively (Figs. 4–6, S2 and S3). Our findings suggest that the affinity of SARS-CoV-2 spike for hACE2 was reduced by the presence of the individual R454G, Y449F, R403G, or N439I mutations and N440I site was critical to the RBD structure. These results are highly consistent with the GST pull-down assay and confirm that the three amino acid residues 454R, 449Y, and 403R are critical for SARS-CoV-2 spike RBD binding to hACE2. These results are also highly consistent with pseudotyped virus infection assay and confirm that the five amino acid residues 454R, 449Y, 403R, 439N and 440N are critical for high infectivity of SARS-CoV-2.

3.5. *Cephalosporin derivative effectively inhibits SARS-CoV-2 spike (WT and variants)-mediated infection and live SARS-CoV-2 infection*

To screen drugs based on interacting with these above key amino acids, molecular docking (Docking) study was performed. As shown in Figs. S4 and S5, 7-Amino cephalosporanic acid, Cefprozil, Ceftazidime or Cefixime can interact with these key amino acids and bind with the SARS-CoV-2 spike RBD. 7-Amino cephalosporanic acid formed structural hydrogen bridge bonds with 496G (Fig. S4C). Cefprozil not only formed hydrogen bridge bonds with 403R and 453Y, but also formed structural hydrogen bridge bonds with 496G (Fig. S4D). Ceftazidime formed hydrogen bridge bonds with 403R and structural hydrogen bridge bonds with 496G (Fig. S5C). Cefixime not only formed hydrogen bridge bonds with 403R, 449Y, 501N, 406E and 498Q, but also formed structural hydrogen bridge bonds with 496G and 505Y (Fig. S5D). The

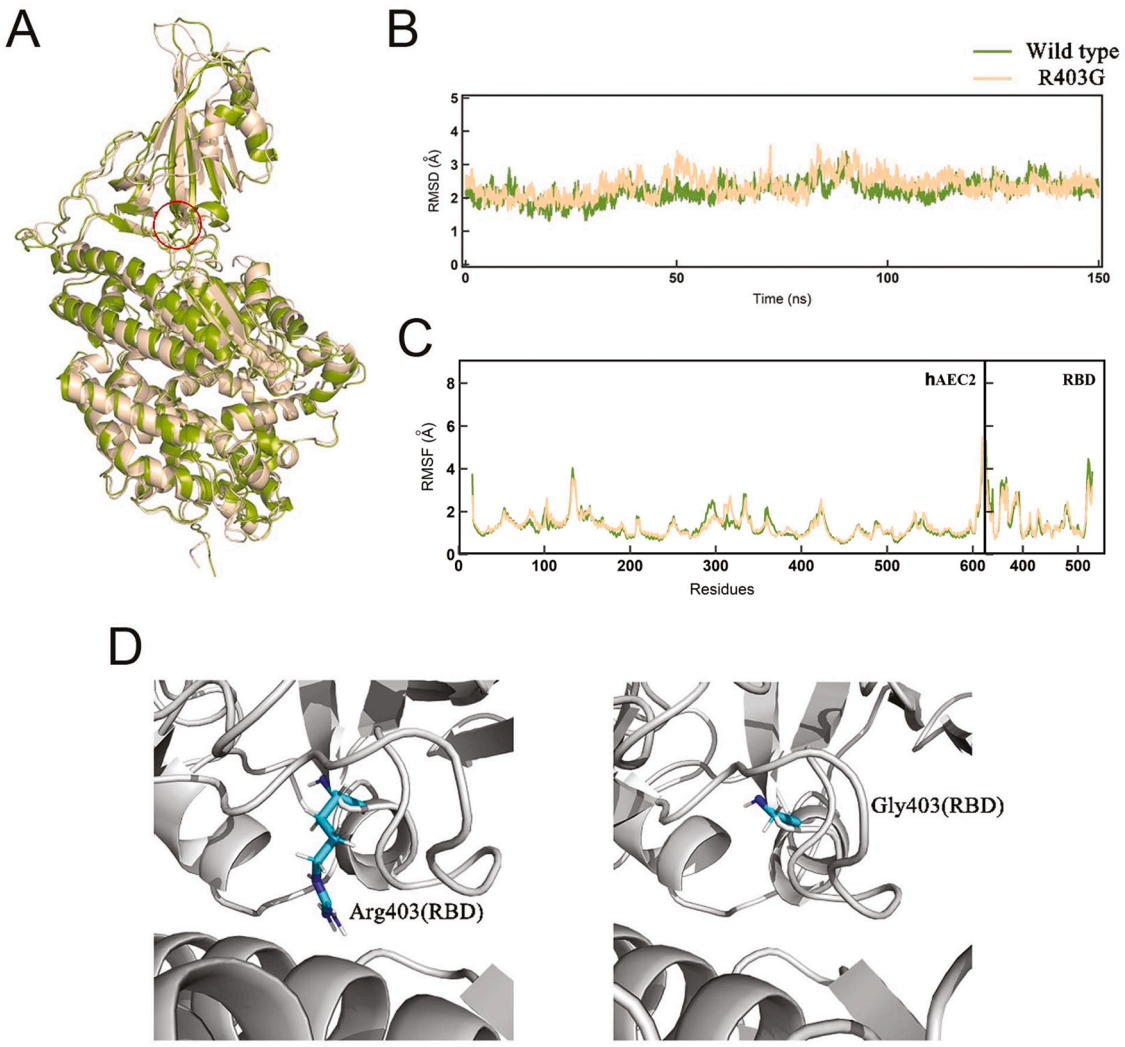

Fig. 6. *MD simulation study of affinity between SARS-CoV-2 spike RBD carrying individual mutation R403G and hACE2.* (A) Average structures in the MD simulation (150 ns). The wildtype SARS-CoV-2 spike RBD is shown in green, and the SARS-CoV-2 spike RBD R403G mutant is shown in wheat. The RMSD between the two complexes is 2.435 Å. The mutant residues are marked with a red circle. (B, C) The RMSD (B) or RMSF (C) of Cα in the MD simulation. (D) The hydrogen bond-based interaction between SARS-CoV-2 spike R403G mutant amino acids and hACE2. In the SARS-CoV-2 spike RBD R403G mutant, no hydrogen bonds are formed with hACE2, and the total binding energy of hACE2 and the SARS-CoV-2 spike RBD R403G mutant is −33.41 ± 0.24 kcal/mol.

total binding energy of Ceftazidime and SARS-CoV-2 spike RBD was -3.8712 kcal/mol. The total binding energy of Cefixime and SARS-CoV-2 spike RBD was -5.3544 kcal/mol.

Before evaluating the antiviral effect of Cephalosporin derivative (7-Amino cephalosporanic acid, Cefprozil, Cefixime or Ceftazidime), we examined whether they affect the viability of 293T-hACE2 used in this study. As shown in Fig. S6, Cephalosporin derivative (7-Amino cephalosporanic acid, Cefprozil, Cefixime or Ceftazidime) had no cytotoxicity to the cells at the dilutions used in the experiments. Next, pseudoviruses bearing SARS-CoV-2 spike were co-incubated with or without Cephalosporin derivative (7-Amino cephalosporanic acid, Cefprozil, Cefixime or Ceftazidime) at different concentrations. As shown in Figs. 7 and 8, 7-Amino cephalosporanic acid (800 μM) significantly inhibited SARS-CoV-2 emerged variants (SA-B.1.351, DELTA-B.1.617, DELTA-B.1.617.2) Spike-mediated pseudovirus infection of 293T-hACE2; Cefprozil (200 μM) significantly inhibited SARS-CoV-2 emerged variants (BZ-P.1, D614G, SA-B.1.351, DELTA-B.1.617, DELTA-B.1.617.2, DELTA-B.1.618) Spike-mediated pseudovirus infection of 293T-hACE2; Cefixime or Ceftazidime dose-dependently and significantly inhibited SARS-CoV-2 wild type or newly emerged variants (BZ-P.1, D614G, GB-B.1.117, SA-B.1.351, DELTA-B.1.617, DELTA-B.1.617.1, DELTA-B.1.617.2, DELTA-B.1.618) Spike-mediated pseudovirus infection of 293T-hACE2.

To further determine the significance of anti-SARS-CoV-2 activity of Cefixime, we examined the efect of Cefixime on live SARS-CoV-2 infection of Vero-E6 cells. Culture supernatant was collected after live SARS-CoV-2 infection. We showed that Cefixime treated cells had significantly decreased expression of viral N gene (Fig. 8J) than the untreated cells. Furthermore, we tested the binding affinity of His-tagged SARS-CoV-2 spike RBD to hACE2 receptor of the host cells treated with or without Cefixime by performing immunofluorescence and western blot analysis. Immunofluorescence assay showed that Cefixime reduced the binding of RBD to hACE2 (Fig. S7A). Consistent with the findings from the immunofluorescence assay, western bolt assay confirmed that Cefixime could block the binding of RBD to hACE2 in a dose-dependent manner (Fig. S7B). In addition, we tested the binding kinetics of Cefixime to RBD by using Surface plasmon resonance and the KD (M) is 2.61×10^{-2}(Fig. S7C). These results indicate that Cefixime and Ceftazidime were identified as potential candidates (novel, safe, and cost-effective drugs) for the prevention/treatment of SARS-CoV-2 wild type and newly emerged variants.

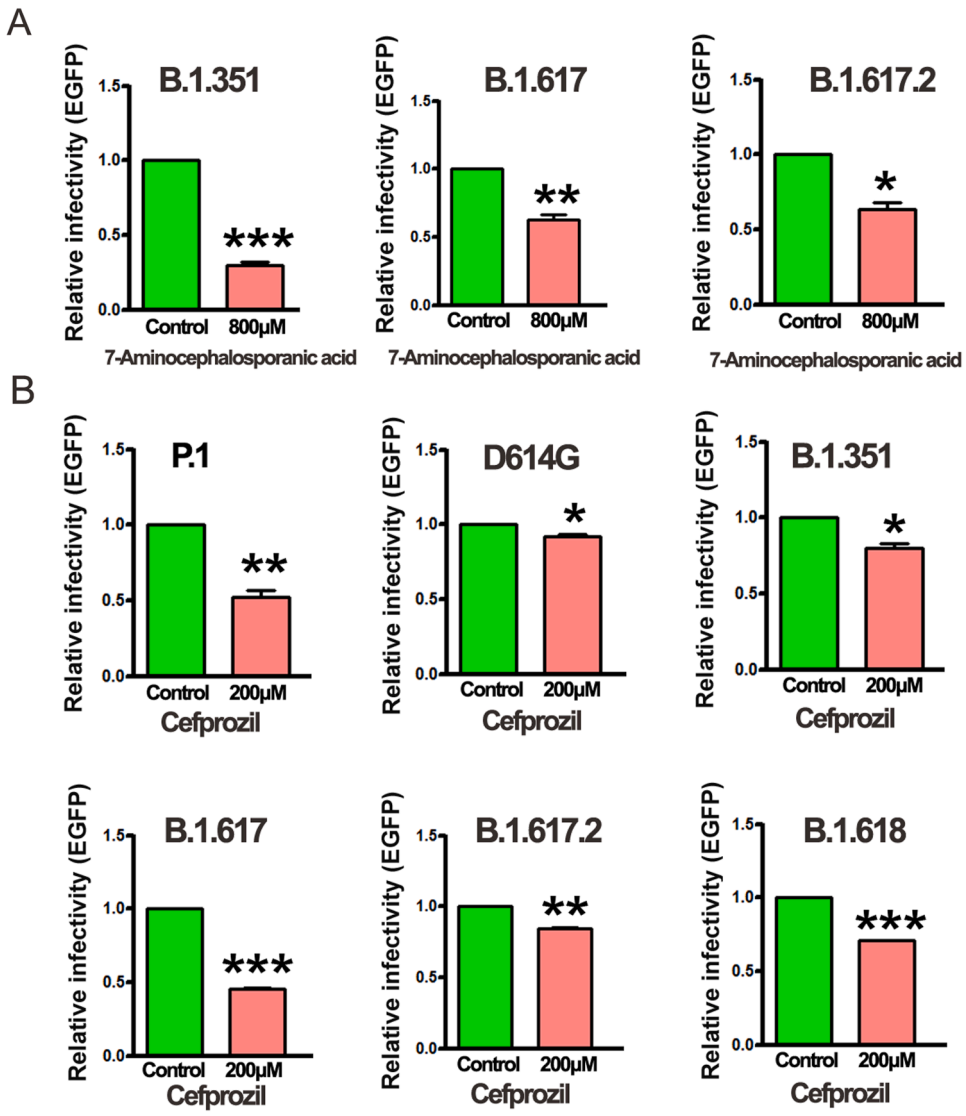

Fig. 7. *7-Amino cephalosporanic acid or Cefprozil inhibited SARS-CoV-2 spike (WT and variants)-mediated infection.* 293T-hACE2 cells were treated with the indicated dose of 7-Amino cephalosporanic acid or Cefprozil and infected with the pseudovirus bearing SARS-CoV-2 spike (WT and variants). The number of EGFP-positive cells was counted by flow cytometry, and the results were used to calculate the infection ability of the pseudotyped viruses.

4. Discussion

The key structure of the interface between the spike protein of SARS-CoV-2 and hACE2 acts as an vital switch for cell entry by the virus during infection (Wang et al., 2020; Letko et al., 2020; Hoffmann et al., 2020). Revealing these interactions is of unquestionable importance for developing COVID-19 vaccines and therapeutics. Here, we identified the RBD2 peptide (391–465 aa) in SARS-CoV-2 spike RBD was required for RBD binding to hACE2. Furthermore, we identified three essential amino acid residues (454R, 449Y, 403R) within the peptide that are critical for its binding to hACE2. By using pseudotyped viruses, we found that virus containing SARS-CoV-2 spike with R454G, Y449F, R403G, N439I or N440I individual mutation has much lower infectivity than virus containing spike protein from the reference strain Wuhan 1 does. Next, Cephalosporin derivative (7-Amino cephalosporanic acid, Cefprozil, Cefixime or Ceftazidime) was found to effectively and significantly block infection of SARS-CoV-2 wild type or newly emerged variants (BZ-P.1, D614G, GB-B.1.117, SA-B.1.351, DELTA-B.1.617, DELTA-B.1.617.1, DELTA-B.1.617.2, DELTA-B.1.618) Spike-mediated pseudovirus infection of 293T-hACE2 by binding with key amino acids for interaction between Spike RBD and hACE2.

We firstly dissected RBD into β-sheets and α-helices based on its structure and constructed the RBD fragments as 319–390, 391–465 and 466–546. Our research indicated that RBD fragment 391–465 (two β-sheets and three α-helices) are required for RBD binding to hACE2. So we chose this fragment 391–465 as our research object. The roles of residues of 466–546 in RBD binding to hACE2 depends on the second structure of 391–465 (two β-sheets and three α-helices). So some residues known to be important in the variants of concern (for instance 484 and 501 (Mannar et al. 2021) were in this way not taken into account.

Thomson et al. (2021) reported that N439K creates a new RBD: hACE2 salt bridge and enhances RBD:hACE2 affinity than wild type . Augusto et al. (2022) reported that N440K mutation enhances the affinity of RBD for hACE2 than wild type. So the 440K and 439K plays critical roles in the affinity of RBD for hACE2. Our research found that N439I and N440I mutations renders SARS-CoV-2 pseudovirus unable to infect hACE2-293T cells. These results indicate that different amino acids at the two sites leads to loss or gain function of spike protein.

Another important finding from the present work is that the 449Y, 403R, 439N or 440N sites in the SARS-CoV-2 spike may be important for the transmission of COVID-19 from intermediate hosts to humans or for increasing COVID-19 transmissibility in humans. Using protein-protein

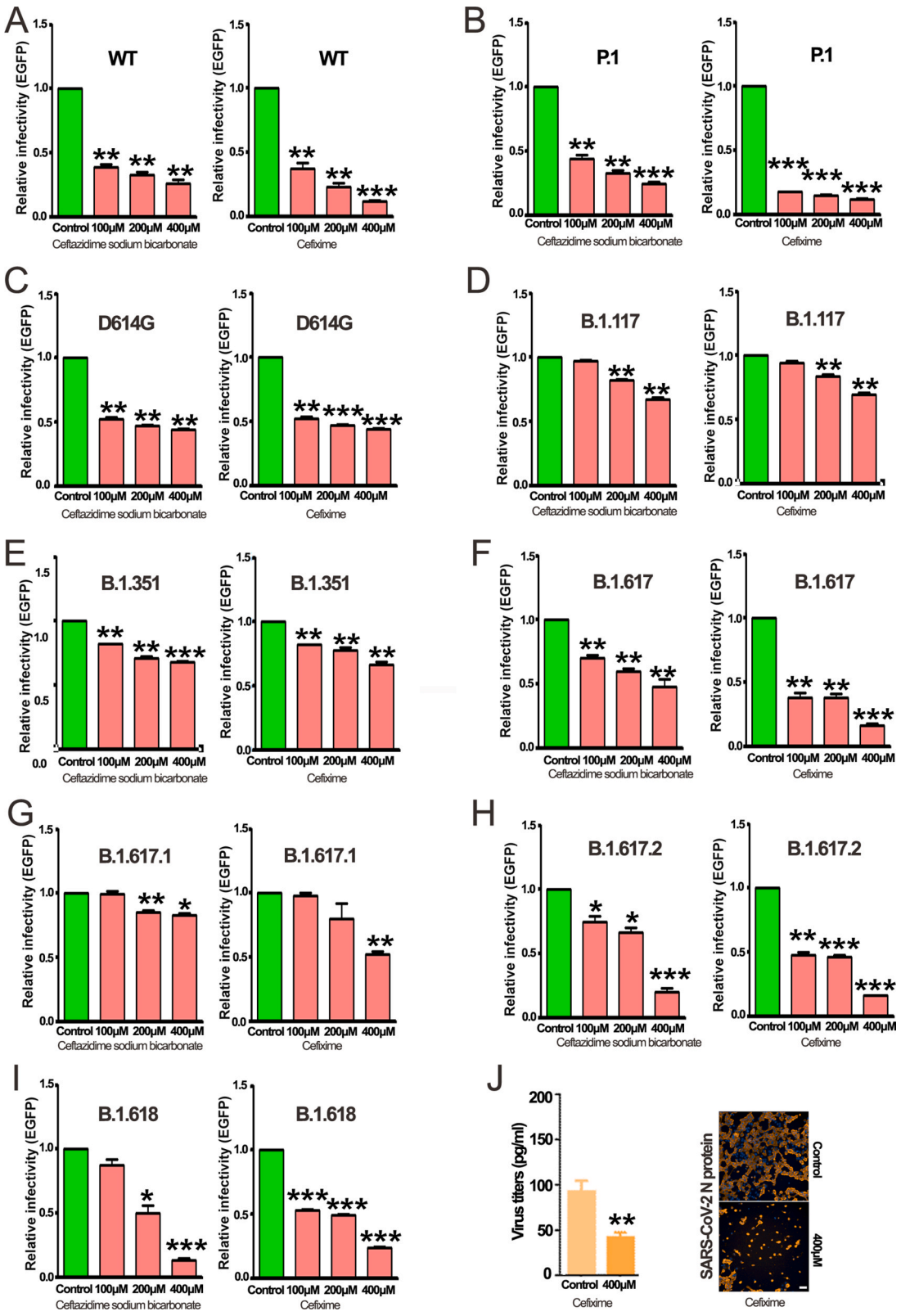

Fig. 8. Ceftazidime or Cefixime inhibited SARS-CoV-2 spike (WT and variants)-mediated infection and live SARS-CoV-2 infection. (A–I)293T-hACE2 cells were treated with the indicated doses of Ceftazidime or Cefixime and infected with the pseudovirus bearing SARS-CoV-2 spike (WT and variants). The number of EGFP-positive cells was counted by flow cytometry, and the results were used to calculate the infection ability of the pseudotyped viruses. (J) Human Vero-E6 were treated with Cefixime (400 μM) before live SARS-CoV-2 infection at MOI = 0.01. Cells were washed 3 times with PBS to remove free virus at 2 h post-infection, and then maintained in DMEM containing Cefixime (400 μM) and 2% FBS for 48 h. Supernatants were collected and SARS-CoV-2 copies were measured by the qRT-PCR for the viral N gene expression (left panel). Immunofluorescence assay was used to detect the expression of N protein and the result was analysised by high content screening (right panel) (Bar = 50 μm).

BLAST, we identified several amino acid differences (403R, 439N, 440N, 449Y, and 459S) between the SARS-CoV-2 reference strain Wuhan 1 RBD2 peptide (391–465 aa) and the corresponding RaTG13 protein sequence. We performed GST pull-down assays and found that two of the above five amino acid residues (449Y, 403R) were critical for SARS-CoV 2 spike RBD–hACE2 interaction. RaTG13 is considered one of the most likely origins of SARS-CoV-2. Therefore, these findings may also help explore the intermediate hosts or origins of SARS-CoV-2.

Our study has some limitations. Recently, studies have identified multiple variants in the SARS-CoV-2 spike RBD (e.g., D614G+V341I, D614G+K458R, and D614G+I472V) that are associated with increased viral infectivity or decreased viral sensitivity to neutralizing monoclonal antibodies (Alouane et al., 2020). This study does not cover all SARS-CoV-2 variants (Groves et al., 2021). Thus, identifying more conserved and variable regions of the virus in further studies could help guide the design of vaccines and drugs.

5. Conclusions

We identified the SARS-CoV-2 spike RBD2 peptide 391–465 aa was required for RBD interacting to hACE2 and three essential amino acid residues (454R, 449Y, and 403R) of spike RBD are critical for its binding to hACE2. Spike 454R, 449Y, 403R, 439N and 440N are critical for infectivity of SARS-CoV-2. These results provide a novel model for drug screening. These results also support further clinical evaluation and development of Cephalosporin derivatives and peptide 391–465 aa of RBD as novel, safe, and cost-effective drugs for prevention/treatment of SARS-CoV-2.

CRediT authorship contribution statement

Xiaopeng Hu: Conceptualization, Methodology, Investigation, Writing – original draft, Writing – review & editing, Project administration, Funding acquisition, Visualization, Supervision. **Jiahua Cui:** Methodology, Investigation, Writing – original draft, Software, Visualization. **Jun Chen:** Methodology, Investigation, Writing – original draft, Software, Visualization. **Shujuan Du:** Methodology, Investigation. **Xinyu Wang:** Methodology, Investigation. **Yabin Zhang:** Investigation. **Jiajun Qian:** Investigation, Writing – original draft, Software. **Haifeng Chen:** Methodology. **Fang Wei:** Supervision. **Qiliang Cai:** Supervision. **Jinping Jia:** Supervision. **Ji Wu:** Writing – review & editing, Project administration, Funding acquisition, Supervision.

Declaration of Competing Interest

The authors declare no competing interests.

Data availability

No data was used for the research described in the article.

Acknowledgment

We would like to thank Prof. Shengce Tao of Shanghai JiaoTong University and Prof. Pei-hui Wang of Shandong University for providing RBD and pGEX-4T-1 plasmid.

Data and materials availability

All data needed to evaluate the conclusions in the paper are present in the paper and/or the Supplementary Materials.

Funding

This work was supported by the China Postdoctoral Science Foundation New Pneumonia Special Project (Grant number 2020T130076ZX), the National Major Scientific Instruments and Equipment Development Project, National Natural Science Foundation of China (61827814).

Consent for publication

Not applicable.

Ethics approval and consent to participate

Not applicable.

Supplementary materials

Supplementary material associated with this article can be found, in the online version, at doi:10.1016/j.virusres.2022.198915.

References

Alouane, T., Laamarti, M., Essabbar, A., Hakmi, M., Bouricha, E.M., Chemao-Elfihri, M. W., Kartti, S., Boumajdi, N., Bendani, H., Laamarti, R., et al., 2020. Genomic diversity and hotspot mutations in 30,983 SARS-CoV-2 genomes: moving toward a universal vaccine for the "confined virus"? Pathogens 9 (10), 1–19.

Arthur, M., McAdoo, M., Guerra, J., Maloney, R., McCluskey, D., Giguere, G., Gomez, G., Collins, J.J., 1996. Clinical comparison of cefuroxime Axetil with Cefixime in the treatment of acute bronchitis. Am. J. Ther. 3 (9), 622–629.

Augusto, G., Mohsen, M.O., Zinkhan, S., Liu, X., Vogel, M., Bachmann, M.F., 2022. *In vitro* data suggest that Indian delta variant B.1.617 of SARS-CoV-2 escapes neutralization by both receptor affinity and immune evasion. Allergy 77 (1), 111–117.

Bain, A.L., Harris, J.L., Khanna, K.K., 2017. Identification of ATM-interacting proteins by co-immunoprecipitation and Glutathione-S-Transferase (GST) pull-down assays. Methods Mol. Biol. 1599, 163–181.

Baum, A., Ajithdoss, D., Copin, R., Zhou, A., Lanza, K., Negron, N., Ni, M., Wei, Y., Mohammadi, K., Musser, B., et al., 2020. REGN-COV2 antibodies prevent and treat SARS-CoV-2 infection in rhesus macaques and hamsters. Science 370 (6520), 1110–1115.

Bluestone, C.D., 1993. Review of Cefixime in the treatment of otitis media in infants and children. Pediatr. Infect. Dis. J. 12 (1), 75–82.

Bosch, B.J., van der Zee, R., de Haan, C.A., Rottier, P.J., 2003. The coronavirus spike protein is a class I virus fusion protein: structural and functional characterization of the fusion core complex. J. Virol. 77 (16), 8801–8811.

Case, D.A., Ben-Shalom, I.Y., Brozell, S.R., Cerutti, D.S., Cheatham III, T.E., Cruzeiro, V. W.D., Darden, T.A., Duke, R.E., Ghoreishi, D., et al., 2018. AMBER 2018. University of California, San Francisco.

Chan, J.F., Yuan, S., Kok, K.H., To, K.K., Chu, H., Yang, J., Xing, F., Liu, J., Yip, C.C., Poon, R.W., et al., 2020. A familial cluster of pneumonia associated with the 2019 novel coronavirus indicating person-to-person transmission: a study of a family cluster. Lancet 395 (10223), 514–523.

Chan, K.K., Dorosky, D., Sharma, P., Abbasi, S.A., Dye, J.M., Kranz, D.M., Herbert, A.S., Procko, E., 2020. Engineering human ACE2 to optimize binding to the spike protein of SARS coronavirus 2. Science 369 (6508), 1261–1265.

Chowdhury, S.M., Talukder, S.A., Khan, A.M., Afrin, N., Ali, M.A., Islam, R., Parves, R., Al Mamun, A., Sufian, M.A., Hossain, M.N., et al., 2020. Antiviral peptides as promising therapeutics against SARS-CoV-2. J. Phys. Chem. B 124 (44), 9785–9792.

Cui, J., Meng, Q., Zhang, X., Cui, Q., Zhou, W., Li, S., 2015. Design and synthesis of new alpha-naphthoflavones as Cytochrome P450 (CYP) 1B1 inhibitors to overcome Docetaxel-resistance associated with CYP1B1 overexpression. J. Med. Chem. 58 (8), 3534–3547.

Darden, T., York, D., Pedersen, L., 1993. Particle mesh Ewald: an N·log(N) method for Ewald sums in large systems. J. Chem. Phys. 98 (12), 10089–10092.

Dong, J., Huang, G., Cui, Q., Meng, Q., Li, S., Cui, J., 2021. Discovery of heterocycle-containing alpha-naphthoflavone derivatives as water-soluble, highly potent and selective CYP1B1 inhibitors. Eur. J. Med. Chem. 209, 112895.

Groves, D.C., SL, R.J., Angyal, A., 2021. The D614G mutations in the SARS-CoV-2 spike protein: implications for viral infectivity, disease severity and vaccine design. Biochem. Biophys. Res. Commun. 538, 104–107.

Hoffmann, M., Kleine-Weber, H., Schroeder, S., Kruger, N., Herrler, T., Erichsen, S., Schiergens, T.S., Herrler, G., Wu, N.H., Nitsche, A., et al., 2020. SARS-CoV-2 cell entry depends on ACE2 and TMPRSS2 and is blocked by a clinically proven protease inhibitor. Cell 181 (2), 271–280 e278.

Huang, C., Wang, Y., Li, X., Ren, L., Zhao, J., Hu, Y., Zhang, L., Fan, G., Xu, J., Gu, X., et al., 2020. Clinical features of patients infected with 2019 novel coronavirus in Wuhan, China. Lancet 395 (10223), 497–506.

Ju, B., Zhang, Q., Ge, J., Wang, R., Sun, J., Ge, X., Yu, J., Shan, S., Zhou, B., Song, S., et al., 2020. Human neutralizing antibodies elicited by SARS-CoV-2 infection. Nature 584 (7819), 115–119.

Khelfaoui, H., Harkati, D., Saleh, B.A., 2021. Molecular docking, molecular dynamics simulations and reactivity, studies on approved drugs library targeting ACE2 and SARS-CoV-2 binding with ACE2. J. Biomol. Struct. Dyn. 39 (18), 7246–7262.
Lan, J., Ge, J., Yu, J., Shan, S., Zhou, H., Fan, S., Zhang, Q., Shi, X., Wang, Q., Zhang, L., et al., 2020. Structure of the SARS-CoV-2 spike receptor-binding domain bound to the ACE2 receptor. Nature 581 (7807), 215–220.
Letko, M., Marzi, A., Munster, V., 2020. Functional assessment of cell entry and receptor usage for SARS-CoV-2 and other lineage B betacoronaviruses. Nat. Microbiol. 5 (4), 562–569.
Li, Q., Guan, X., Wu, P., Wang, X., Zhou, L., Tong, Y., Ren, R., Leung, K.S.M., Lau, E.H.Y., Wong, J.Y., et al., 2020. Early transmission dynamics in Wuhan, China, of novel coronavirus-infected pneumonia. N. Engl. J. Med. 382 (13), 1199–1207.
Li, Q., Wu, J., Nie, J., Zhang, L., Hao, H., Liu, S., Zhao, C., Zhang, Q., Liu, H., Nie, L., et al., 2020. The impact of mutations in SARS-CoV-2 spike on viral infectivity and antigenicity. Cell 182 (5), 1284–1294 e1289.
Li, F., 2016. Structure, function, and evolution of coronavirus spike proteins. Ann. Rev. Virol. 3 (1), 237–261.
Lin, C., Li, Y., Zhang, Y., Liu, Z., Mu, X., Gu, C., Liu, J., Li, Y., Li, G., Chen, J., 2021. Ceftazidime is a potential drug to inhibit SARS-CoV-2 infection *in vitro* by blocking spike protein-ACE2 interaction. Signal Transduct. Target. Ther. 6 (1), 198.
Liu, J., Bodnar, B.H., Meng, F., Khan, A.I., Wang, X., Saribas, S., Wang, T., Lohani, S.C., Wang, P., Wei, Z., et al., 2021. Epigallocatechin gallate from green tea effectively blocks infection of SARS-CoV-2 and new variants by inhibiting spike binding to ACE2 receptor. Cell Biosci. 11 (168), 1–15.
Liu, H., Ye, W., Chen, H.F., 2017. Positive cooperative regulation of double binding sites for human acetylcholinesterase. Chem. Biol. Drug Des. 89 (5), 694–704.
Lv, M., Luo, X., Estill, J., Liu, Y., Ren, M., Wang, J., Wang, Q., Zhao, S., Wang, X., Yang, S., et al., 2020. Coronavirus disease (COVID-19): a scoping review. Eur. Commun. Dis. Bull. 25 (15), 25.
Maier, J.A., Martinez, C., Kasavajhala, K., Wickstrom, L., Hauser, K.E., Simmerling, C., 2015. ff14SB: improving the accuracy of protein side chain and backbone parameters from ff99SB. J. Chem. Theor. Comput. 11 (8), 3696–3713.
Mannar, D., Saville, J.W., Zhu, X., Srivastava, S.S., Berezuk, A.M., Zhou, S., Tuttle, K.S., Kim, A., Li, W., Dimitrov, D.S., et al., 2021. Structural analysis of receptor binding domain mutations in SARS-CoV-2 variants of concern that modulate ACE2 and antibody binding. Cell Rep. 37 (12), 110156.
Nag, A., Paul, S., Banerjee, R., Kundu, R., 2021. In silico study of some selective phytochemicals against a hypothetical SARS-CoV-2 spike RBD using molecular docking tools. Comput. Biol. Med. 137, 104818.
Nie, J., Li, Q., Wu, J., Zhao, C., Hao, H., Liu, H., Zhang, L., Nie, L., Qin, H., Wang, M., et al., 2020. Establishment and validation of a pseudovirus neutralization assay for SARS-CoV-2. Emerg. Microbes Infect. 9 (1), 680–686.
Pan, Y., Du, J., Liu, J., Wu, H., Gui, F., Zhang, N., Deng, X., Song, G., Li, Y., Lu, J., et al., 2021. Screening of potent neutralizing antibodies against SARS-CoV-2 using convalescent patients-derived phage-display libraries. Cell Discov. 7 (1), 57.
Perlman, S., Netland, J., 2009. Coronaviruses post-SARS: update on replication and pathogenesis. Nat. Rev. Microbiol. 7 (6), 439–450.
Pinto, D., Park, Y.J., Beltramello, M., Walls, A.C., Tortorici, M.A., Bianchi, S., Jaconi, S., Culap, K., Zatta, F., De Marco, A., et al., 2020. Cross-neutralization of SARS-CoV-2 by a human monoclonal SARS-CoV antibody. Nature 583 (7815), 290–295.
Quintiliani, R., 1996. Cefixime in the treatment of patients with lower respiratory tract infections: results of US clinical trials. Clin. Ther. 18 (3), 373–390 discussion 372.
Rashid, H.U., Ahmad, N., Abdalla, M., Khan, K., Martines, M.A.U., Shabana, S., 2022. Molecular docking and dynamic simulations of Cefixime, Etoposide and Nebrodenside A against the pathogenic proteins of SARS-CoV-2. J. Mol. Struct. 1247, 131296.
Ryckaert, J.P., Ciccotti, G., Berendsen, H.J.C., 1977. Numerical integration of the Cartesian equations of motion of a system with constraints: molecular dynamics of n-alkanes. J. Comput. Phys. 23 (3), 327–341.
Shang, J., Ye, G., Shi, K., Wan, Y., Luo, C., Aihara, H., Geng, Q., Auerbach, A., Li, F., 2020. Structural basis of receptor recognition by SARS-CoV-2. Nature 581 (7807), 221–224.
Sharma, K.K., Wang, Z., Motola, D.L., Cummins, C.L., Mangelsdorf, D.J., Auchus, R.J., 2009. Synthesis and activity of dafachronic acid ligands for the C. elegans DAF-12 nuclear hormone receptor. Mol. Endocrinol. 23 (5), 640–648.
Shirley, M., 2018. Ceftazidime-avibactam: a review in the treatment of serious gram-negative bacterial infections. Drugs 78 (6), 675–692.
Sohrabi, C., Alsafi, Z., O'Neill, N., Khan, M., Kerwan, A., Al-Jabir, A., Iosifidis, C., Agha, R., 2020. World Health Organization declares global emergency: a review of the 2019 novel coronavirus (COVID-19). Int. J. Surg. 76, 71–76.
Song, D., Luo, R., Chen, H.F., 2017. The IDP-specific force field ff14IDPSFF improves the conformer sampling of intrinsically disordered proteins. J. Chem. Inf. Model. 57 (5), 1166–1178.
Teixeira, L.M.C., Coimbra, J.T.S., Ramos, M.J., Fernandes, P.A., 2022. Transmembrane protease serine 2 proteolytic cleavage of the SARS-CoV-2 spike protein: a mechanistic quantum mechanics/molecular mechanics study to inspire the design of new drugs to fight the COVID-19 pandemic. J. Chem. Inf. Model. 62 (10), 2510–2521.
Thomson, E.C., Rosen, L.E., Shepherd, J.G., Spreafico, R., da Silva Filipe, A., Wojcechowskyj, J.A., Davis, C., Piccoli, L., Pascall, D.J., Dillen, J., et al., 2021. Circulating SARS-CoV-2 spike N439K variants maintain fitness while evading antibody-mediated immunity. Cell 184 (5), 1171–1187 e1120.
Vilar, S., Cozza, G., Moro, S., 2008. Medicinal chemistry and the molecular operating environment (MOE): application of QSAR and molecular docking to drug discovery. Curr. Top. Med. Chem. 8 (18), 1555–1572.
Walls, A.C., Park, Y.J., Tortorici, M.A., Wall, A., McGuire, A.T., Veesler, D., 2020. Structure, function, and antigenicity of the SARS-CoV-2 spike glycoprotein. Cell 183 (6), 1735.
Wang, Q., Zhang, Y., Wu, L., Niu, S., Song, C., Zhang, Z., Lu, G., Qiao, C., Hu, Y., Yuen, K. Y., et al., 2020. Structural and functional basis of SARS-CoV-2 entry by using human ACE2. Cell 181 (4), 894–904 e899.
Wrapp, D., Wang, N., Corbett, K.S., Goldsmith, J.A., Hsieh, C.L., Abiona, O., Graham, B. S., McLellan, J.S., 2020. Cryo-EM structure of the 2019-nCoV spike in the prefusion conformation. Science 367 (6483), 1260–1263.
Yan, R., Zhang, Y., Li, Y., Xia, L., Guo, Y., Zhou, Q., 2020. Structural basis for the recognition of SARS-CoV-2 by full-length human ACE2. Science 367 (6485), 1444–1448.
Yang, X., Yu, Y., Xu, J., Shu, H., Xia, J., Liu, H., Wu, Y., Zhang, L., Yu, Z., Fang, M., et al., 2020. Clinical course and outcomes of critically ill patients with SARS-CoV-2 pneumonia in Wuhan, China: a single-centered, retrospective, observational study. Lancet Respir. Med. 8 (5), 475–481.
Yi, C., Sun, X., Ye, J., Ding, L., Liu, M., Yang, Z., Lu, X., Zhang, Y., Ma, L., Gu, W., et al., 2020. Key residues of the receptor binding motif in the spike protein of SARS-CoV-2 that interact with ACE2 and neutralizing antibodies. Cell. Mol. Immunol. 17 (6), 621–630.
Zhou, P., Yang, X.L., Wang, X.G., Hu, B., Zhang, L., Zhang, W., Si, H.R., Zhu, Y., Li, B., Huang, C.L., et al., 2020. A pneumonia outbreak associated with a new coronavirus of probable bat origin. Nature 579 (7798), 270–273.